

# Gas-phase conversion of glycerol to synthesis gas over carbon-supported platinum and platinum–rhenium catalysts

D.A. Simonetti, E.L. Kunkes, J.A. Dumesic \*

*Department of Chemical and Biological Engineering, 1415 Engineering Drive, University of Wisconsin, Madison, WI 53706, USA*

Received 15 December 2006; revised 29 January 2007; accepted 30 January 2007

Available online 21 March 2007

---

## Abstract

The rate of glycerol conversion to H<sub>2</sub>/CO gas mixtures was measured under kinetically controlled reaction conditions over carbon-supported platinum and platinum–rhenium catalysts. The reaction is fractional order with respect to glycerol and zero order with respect to hydrogen, with activation barriers of 60–90 kJ mol<sup>−1</sup>. The addition of an equimolar amount of Re to Pt/C increases the production rate of CO by a factor of 5 at low conversion (<20%) and while co-feeding H<sub>2</sub>, both of these factors leading to low pressures of CO in the reactor. At higher conversion conditions (20% conversion to gas-phase products) and without co-feeding H<sub>2</sub>, the Pt–Re/C catalyst is an order of magnitude more active than Pt/C. Accordingly, Re has a greater promotional effect on the rate of glycerol conversion at conditions leading to higher CO pressures, suggesting that the primary promotional effect of Re is to weaken the interaction of CO with the surface, thereby decreasing the CO coverage and allowing the catalyst to operate at high rates in the presence of gaseous CO. Temperature-programmed reduction (TPR) studies of carbon-supported Pt and Re catalysts showed a peak near 460 K for Pt/C and near 650 K for Re/C. The position of the TPR peak for Re shifted to lower temperature on addition of Pt to Re, suggesting interaction between Pt and Re species, leading to alloy formation.

© 2007 Elsevier Inc. All rights reserved.

**Keywords:** Synthesis gas; Platinum; Rhenium; Glycerol; Carbon-supported catalysts

---

## 1. Introduction

The development of alternative sources of energy is becoming important in this era of diminishing petroleum reserves and increased environmental awareness. Biomass is an intriguing candidate in this respect, because it is renewable and its consumption is neutral with respect to greenhouse gas emissions [1]. Hydrogen can be produced from oxygenated hydrocarbons via aqueous-phase reforming [2–8] or from other biomass feedstocks via steam reforming and gasification [9–12]. Steam gasification of biomass can also produce synthesis gas, which can be used in the Fischer–Tropsch synthesis reaction to produce liquid fuels [13,14]. Liquid fuels and light alkanes also can be produced from oxygenated hydrocarbons via aqueous-phase dehydration/hydrogenation [15,16], and biodiesel is pro-

duced from the transesterification of plant oils and animal fats [1].

Recently, we have reported a low-temperature (e.g., 550 K) catalytic process that converts glycerol (derived as, e.g., a byproduct of biodiesel production) into H<sub>2</sub>/CO gas mixtures [17]. Because this production of synthesis gas can be accomplished in the same temperature range as Fischer–Tropsch synthesis, the endothermic production of synthesis gas at low temperatures can be coupled with exothermic Fischer–Tropsch synthesis, leading to an energy-integrated process for conversion of biomass to liquid transportation fuels. In the present paper, we report results of reaction kinetics and catalyst characterization measurements for the conversion of glycerol to synthesis gas over various Pt-based catalysts.

The conversion of glycerol to H<sub>2</sub> and CO takes place according to the following stoichiometric equation:



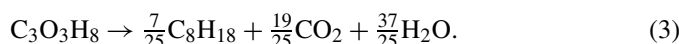
\* Corresponding author. Fax: +1 608 262 0832.

E-mail address: [dumesic@engr.wisc.edu](mailto:dumesic@engr.wisc.edu) (J.A. Dumesic).

The H<sub>2</sub>:CO ratio for the above reaction is equal to 1.33. This ratio can be increased by the water–gas shift (WGS) reaction:



The stoichiometry for conversion of glycerol to liquid alkanes, by the formation of synthesis gas coupled with Fischer–Tropsch synthesis, is



This overall reaction to produce liquid fuels from glycerol is slightly exothermic, such that 96% of the energy content of the glycerol molecule is retained in the liquid alkane product [17].

In previous work, we tested various supported Pt catalysts for glycerol conversion and found that Pt supported on carbon gave the best activity, stability, and selectivity to H<sub>2</sub>/CO at temperatures near 620 K. However, the activity of Pt/C is low at temperatures below 570 K, most likely related to high surface coverage by adsorbed CO [17]. Because Fischer–Tropsch synthesis is typically carried out in the temperature range of 470–550 K [18], it was necessary to find a catalyst that operates at these low temperatures so that heat integration is possible between the synthesis gas production and utilization steps. In this respect, it was found that a carbon-supported Pt–Re catalyst with an atomic Pt:Re ratio of 1:1 gave high activity, stability, and selectivity to H<sub>2</sub>/CO in the desired temperature range [17].

In the present paper, we report results of experimental studies to measure the intrinsic rates of synthesis gas production from glycerol over carbon-supported Pt and Pt–Re catalysts. We conducted reaction kinetics measurements at various temperatures and different inlet partial pressures of glycerol, H<sub>2</sub>O, and H<sub>2</sub> over catalysts with varying Pt–Re ratios as well as monometallic Pt. We also conducted temperature-programmed reduction (TPR) experiments as well as H<sub>2</sub> and CO chemisorption measurements to investigate the nature of the Pt–Re interaction in the bimetallic catalysts. The results of these reaction kinetics studies show that the reaction is zero order with respect to H<sub>2</sub> and fractional order with respect to glycerol. The activation energy for synthesis gas production was 60–90 kJ mol<sup>−1</sup> for monometallic Pt and Pt–Re bimetallic catalysts. The catalyst with an atomic Pt:Re ratio of 1:1 was 5 times more active than the monometallic Pt catalyst and the Pt–Re catalyst with a ratio of 10:1 under low conversion conditions with H<sub>2</sub> co-feed. At higher conversion to gas phase products, the activity of the Pt–Re/C catalyst was an order of magnitude higher than Pt/C, suggesting that the addition of Re to Pt decreases the extent to which CO inhibits the rate of reaction.

## 2. Experimental

### 2.1. Catalyst preparation

Carbon-supported Pt and Re catalysts were prepared by incipient wetness impregnation of carbon black (Vulcan XC-72) with aqueous solutions of H<sub>2</sub>PtCl<sub>6</sub>·6H<sub>2</sub>O and HReO<sub>4</sub> (Strem Chemicals). The carbon-supported Pt–Re catalysts were prepared by impregnating the support with an aqueous solution of both H<sub>2</sub>PtCl<sub>6</sub>·6H<sub>2</sub>O and HReO<sub>4</sub>. The support was dried in air

for 12 h at 373 K before impregnation, and 1.7 g of solution was used for every gram of support. The catalyst was dried at 403 K for 12 h in air after impregnation.

Before reaction kinetics or gas adsorption measurements (i.e., CO and H<sub>2</sub> chemisorption), the catalysts were reduced in H<sub>2</sub> (180 cm<sup>3</sup>(STP) min<sup>−1</sup>, corresponding to gas hourly space velocities (GHSVs) between 2.0 × 10<sup>3</sup> and 5.0 × 10<sup>4</sup> h<sup>−1</sup>). The GHSV was calculated using the total volumetric flowrate of gas (at standard conditions) into the reactor and a bed density of 0.29 g cm<sup>−3</sup> for undiluted catalyst (chemisorption and TPR experiments) and 0.15 g cm<sup>−3</sup> for catalyst diluted with an equal volume of crushed SiO<sub>2</sub> granules (reaction kinetics experiments). The reactor was heated to 723 K (0.5 K min<sup>−1</sup>) for Pt–Re/C or 533 K (0.5 K min<sup>−1</sup>) for Pt/C and held at this temperature for 2 h. The adsorption uptakes of carbon monoxide and H<sub>2</sub> at 300 K were measured on a standard gas adsorption apparatus described elsewhere [19]. The number of catalytic sites was taken to be equal to the irreversible CO uptake.

### 2.2. TPR

TPR experiments were carried out in an apparatus consisting of a mass flow controller (Teledyne-Hastings) and tube furnace connected to a variable power-supply and PID temperature controller (Love Controls) with a K-type thermocouple (Omega). Dried, unreduced catalyst samples (0.3 g) were loaded into a 12.6-mm (0.5-inch)-o.d. fritted quartz tube reactor. A mixture of 5.18% H<sub>2</sub> in N<sub>2</sub> (Linde) was fed to the reactor at a flow rate of 50 cm<sup>3</sup>(STP) min<sup>−1</sup> (GHSV = 3.0 × 10<sup>3</sup> h<sup>−1</sup>). The sample was heated from room temperature to 973 K at a rate of 10 K min<sup>−1</sup>. Before heating, the sample was exposed to the gas mixture for 30 min at room temperature. The effluent was monitored by a mass spectrometer system consisting of a quadrupole residual gas analyzer (Stanford Instruments RGA 200) inside a vacuum chamber. Vacuum was provided by a diffusion pump connected in series to a rotary pump. The effluent was introduced into the vacuum chamber via a constricted quartz capillary, resulting in a pressure of 5 × 10<sup>−5</sup> Torr inside the chamber.

### 2.3. Reaction kinetics measurements

Fig. 1 shows a schematic diagram of the apparatus used to conduct the reaction kinetics studies of the conversion of glycerol to synthesis gas. The reactor used for studies of glycerol conversion with H<sub>2</sub> co-feed was a 6.3-mm (0.25-inch)-o.d. stainless steel tube with a wall thickness of 0.71 mm (0.028 inch). Reaction kinetics studies using a glycerol/water feed but without gas co-feed were carried out using a stainless steel tubular reactor with a 12.6 mm (0.5 inch) o.d. and a wall thickness of 0.71 mm (0.028 inch). A bed consisting of fresh powder catalyst (30–50 mg for the 6.3-mm reactor; 90–760 mg for the 12.6-mm reactor) mixed with an equal volume of crushed fused SiO<sub>2</sub> granules (to decrease pressure drop across the bed) was loaded between a quartz wool plug and fused SiO<sub>2</sub> granules (−4 + 16 mesh; Sigma Aldrich). The reactor was heated with a furnace consisting of a close-fitting aluminum block heated externally by a well-insulated furnace (1450 W/115 V, Applied

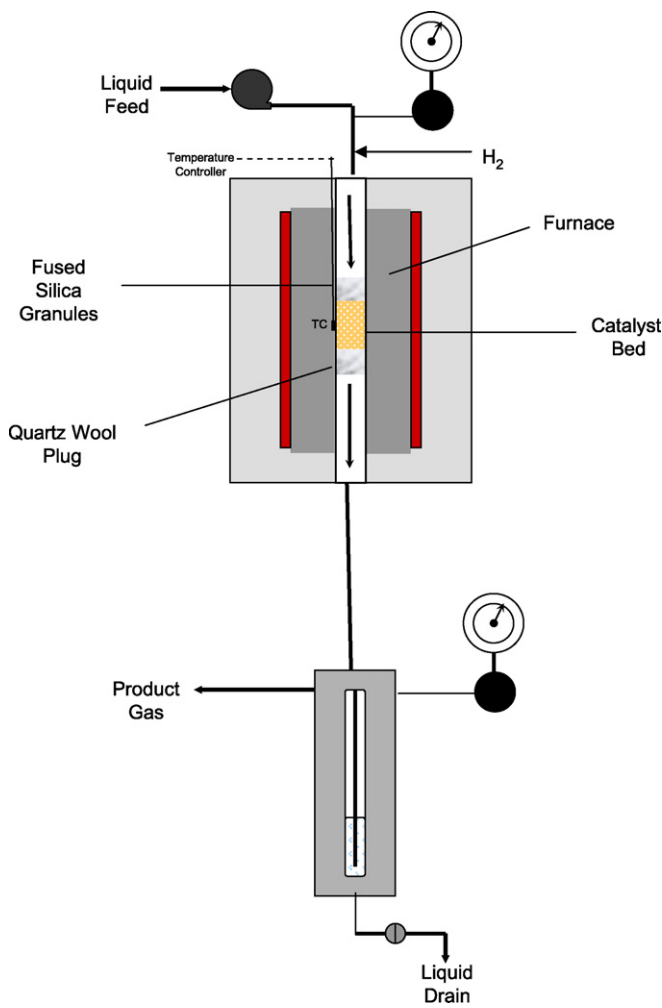


Fig. 1. Schematic diagram of reaction kinetics apparatus.

Test Systems Series 3210). A K-type thermocouple (Omega) was attached to the outside of the reactor to measure temperature, which was controlled with a 1600 series type temperature controller (Dwyer Instruments). Tests were conducted with an internal thermocouple to confirm that the temperature reading at the outside reactor wall was the same as inside the catalyst bed. Solutions of glycerol (99.5+%; Sigma Aldrich) and deionized water were introduced into the reactor, with or without gas co-feed, in a down-flow configuration. The liquid feed flowrate was controlled with an HPLC pump (Alltech Model 301) and entered a syringe needle (Hamilton; point 5 tip) to introduce droplets of the feed into the reactor where vaporization occurs. The flow of carrier gas was controlled with a Brooks Model 5850 mass-flow controller. The glycerol feed concentration, liquid feed flowrate, and H<sub>2</sub> flowrate were adjusted to vary the inlet partial pressure of either glycerol or water while maintaining the inlet partial pressure of the other reactant constant. The partial pressure of hydrogen varies for each reaction condition, because the reaction was found to be zero order with respect to hydrogen (as discussed later). The effluent liquid was condensed in a gas–liquid separator and drained periodically for gas chromatography (GC) analysis with an Agilent 6890 gas chromatograph equipped with a flame-ionization detector

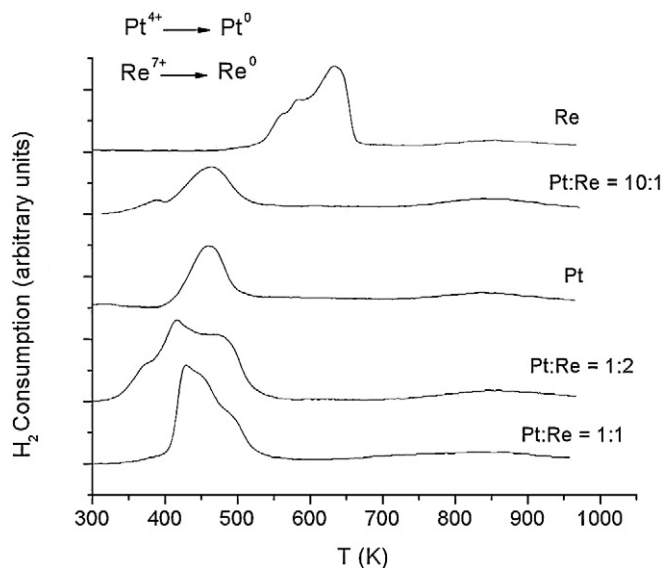


Fig. 2. Temperature-programmed reduction profiles for 5 wt% Pt/C, 5 wt% Re/C, and bimetallic Pt–Re/C catalysts described in Table 1.

(FID) and HP-Innowax column. Each effluent was tested for the presence of glycerol and trace amounts of other liquid byproducts. The effluent gas stream passed through a back-pressure regulator (GO Regulator, Model BP-60) to maintain the system pressure, and the gas was analyzed for CO, CO<sub>2</sub>, and light alkanes (C<sub>1</sub>–C<sub>3</sub>) using an HP-5890 GC with thermal conductivity detector (TCD) and a Haysep DB 100/120 column (Alltech). A Carle GC 8700 with TCD was used to analyze H<sub>2</sub> in the effluent gas. Reaction kinetics data were collected for 2–5 h on stream for each set of reaction conditions to ensure that the catalyst system reached steady state. Replicate runs gave a standard deviation in the CO turnover frequency (TOF) of 4 min<sup>−1</sup> at 548 K and 1 bar total pressure (inlet pressures of 0.06 bar glycerol, 0.72 bar water, balance H<sub>2</sub>).

#### 2.4. X-ray diffraction

X-ray diffraction (XRD) was used to investigate alloy formation for the 10 wt% Pt–Re (atomic Pt:Re = 1:1)/C catalyst. A Scintag PAD V X-ray diffractometer with monochromated CuK<sub>α</sub> X-rays was used in the diffraction studies. The tube voltage and current were 45 kV and 40 mA, respectively. Diffraction patterns were collected in the 2θ range from 30° to 90°, with 0.02° intervals and a dwell time of 2 s. Before diffraction studies, the catalyst samples were reduced in 180 cm<sup>3</sup>(STP) min<sup>−1</sup> H<sub>2</sub> (GHSV = 1.0 × 10<sup>4</sup> h<sup>−1</sup>) at 723 or 973 K and passivated in 180 cm<sup>3</sup>(STP) min<sup>−1</sup> of 2% O<sub>2</sub>/He mixture (GHSV = 1.0 × 10<sup>4</sup> h<sup>−1</sup>).

### 3. Results

#### 3.1. TPR

Fig. 2 shows TPR profiles of 5 wt% Pt/C, 5 wt% Re/C, 10 wt% Pt–Re (atomic Pt:Re = 1:1)/C, 5.6 wt% Pt–Re (10:1)/C, and 10 wt% Pt–Re (1:2)/C, and Table 1 gives the properties

Table 1  
Properties of catalysts

Catalyst	Pt loading (wt%)	Re loading (wt%)	Bulk atomic Pt:Re ratio	Irreversible CO uptake ( $\mu\text{mol g}^{-1}$ )	Irreversible H uptake ( $\mu\text{mol g}^{-1}$ )	CO:(total metal) atomic ratio	CO:H uptake ratio
Re/C	–	5.0	–	30	–	0.10	–
Pt/C	5.0	–	–	130	130	0.53	1.0
Pt/C <sup>a</sup>	5.0	–	–	90	–	0.36	–
Pt–Re/C	5.1	4.9	1:1	150	64	0.29	2.3
Pt–Re/C	5.1	0.5	10:1	120	90	0.40	1.3
Pt–Re/C	3.4	6.6	1:2	64	48	0.12	1.3

<sup>a</sup> Sintered in H<sub>2</sub> at 773 K.

of these catalysts. The reduction profile of Pt/C shows a uniform reduction peak at 460 K, which is accompanied by HCl emission, indicating the decomposition of H<sub>2</sub>PtCl<sub>6</sub>. The Re/C reduction profile consists of a broader peak with a maximum at 640 K. Hydrogen consumption measurements indicate the complete reduction of the Pt<sup>4+</sup> and Re<sup>7+</sup> precursors into Pt<sup>0</sup> and Re<sup>0</sup>, respectively. The addition of small amounts of Re to Pt/C (5.6 wt% Pt–Re (10:1)/C) caused the Pt reduction peak to broaden without affecting the position of the maximum. The addition of larger amounts of Re resulted in a change in peak shape and a shift of the reduction maximum to 431 K for the 10 wt% Pt–Re (1:1) and 417 K for the Pt–Re (1:2) catalysts. The reduction profiles of the bimetallic catalysts do not contain peaks in the same region as 5 wt% Re/C, and these Pt–Re catalysts have hydrogen consumption corresponding to complete reduction of the Pt<sup>4+</sup> and Re<sup>7+</sup> precursors. This behavior demonstrates that the presence of Pt significantly lowers the reduction temperature of the Re precursor. All of the reduction profiles contain a broad hydrogen consumption peak centered at 840–850 K. This peak is accompanied by methane emission and results from hydrogenation of surface functional groups on the carbon support. This gasification of the support is in agreement with the observations of other investigators [20–24].

### 3.2. Chemisorption studies

Table 1 shows the irreversible CO uptakes for monometallic Pt/C and Re/C catalysts along with Pt–Re/C catalysts of varying Pt:Re atomic ratios. The Pt/C catalyst is the most highly dispersed (defined as number of irreversibly adsorbed CO molecules divided by the total number of metal atoms), and the dispersion decreases as the Re content increases. Addition of a small amount of Re (atomic Pt:Re = 10:1) results in a decrease in CO uptake compared with monometallic Pt. However, the catalyst with equal amounts of Pt and Re shows increased CO uptake compared with monometallic Pt. When rhenium is present in excess compared with platinum (Pt–Re (1:2)/C), the dispersion approaches that of the monometallic Re/C catalyst. For both Pt/C and Pt–Re/C, H<sub>2</sub> uptake decreases with the addition of a small amount of Re to Pt (Pt:Re = 10:1). Addition of an equimolar amount of Re to Pt reduces the H<sub>2</sub> uptake by a factor of 2. This result indicates the formation of an alloy in the bimetallic catalysts [25]. Table 1 also shows the CO:H adsorption ratio for each catalyst. This ratio is equal to 1.0 for the Pt/C

catalyst and increases to 2.3 when an equimolar amount of Re is added to Pt.

### 3.3. Reaction kinetics measurements

Reaction kinetics measurements carried out at 548 K and low conversions (i.e., <20%) without a hydrogen co-feed resulted in slow catalyst deactivation (e.g., a first-order deactivation constant equal to 0.02 h<sup>-1</sup>). However, the catalytic activity remained stable with time on stream (for at least 2 days) upon addition of a hydrogen co-feed. This result suggests that hydrogen plays a role in maintaining catalyst stability, possibly by hydrogenating unsaturated coke precursors [17]. Therefore, hydrogen was used as a co-feed, at inlet  $P_{\text{H}_2}:P_{\text{glycerol}}$  partial pressure ratios of between 1 and 3, for all kinetics experiments. We note that slow deactivation was observed when the  $P_{\text{H}_2}:P_{\text{glycerol}}$  partial pressure ratio was <1. Importantly, the rate of CO production was unaffected by the addition of hydrogen, indicating that the overall rate of glycerol conversion is zero order with respect to the hydrogen pressure.

Various dimensionless groups have been developed from theoretical analyses of the influence of heat and mass transport in chemical kinetics measurements [26–34]. These criteria predict that our system is free from such transport limitations. Interphase mass transfer can become limiting for larger catalyst particles; however, maintaining the catalyst particle size below 110  $\mu\text{m}$  should prevent mass transfer limitations for this system. In addition, the Madon–Boudart method was used to test for the presence of transport limitations for the vapor-phase conversion of a 30 wt% glycerol solution to synthesis gas [35]. Two carbon-supported Pt–Re catalysts with different loadings and the same total metal dispersion were prepared. An atomic Pt:Re ratio of 1:1 and a dispersion of 0.29 were maintained for both catalysts. The rate of CO production was measured at 548 K and inlet partial pressures of 0.06 bar for glycerol, 0.72 bar for H<sub>2</sub>O, and 0.22 bar for H<sub>2</sub>, with GHSVs between  $2 \times 10^4$  and  $1 \times 10^5 \text{ h}^{-1}$ . The TOFs are the same (within 10%) for both catalysts (170 min<sup>-1</sup> for the 2 wt% catalyst and 185 min<sup>-1</sup> for the 10 wt% catalyst at 30% conversion to gas-phase products). This result indicates that the Madon–Boudart criterion for the absence of transport limitations is satisfied for catalysts with total metal loading of 2–10 wt% at 548 K. Thus, 5 wt% Pt/C catalysts with loadings of Re of 0–5 wt% were chosen for further study of the intrinsic reaction kinetics for the conversion of glycerol to syn-

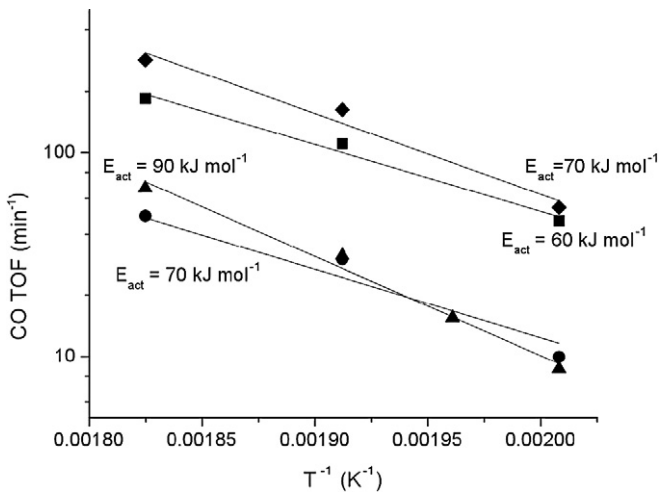


Fig. 3. Turnover frequency as a function of temperature for Pt/C (▲), Pt-Re (10:1)/C (●), Pt-Re (1:1)/C (■), and Pt-Re (1:2)/C (◆) catalysts. Data collected at inlet partial pressures of  $P_{gly} = 0.06$  bar,  $P_{H_2O} = 0.72$  bar, and  $P_{H_2} = 0.22$  bar over 30–50 mg of catalyst (GHSV between  $7 \times 10^4$  and  $1 \times 10^5$   $h^{-1}$ ).

thesis gas. In addition, a catalyst with an atomic Pt:Re ratio of 1:2 (i.e., 6.6 wt% Re and 3.4 wt% Pt) was studied.

To test whether glycerol conversion to synthesis gas is a structure-sensitive reaction, a Pt/C catalyst was sintered, and the rate of CO production was measured at 548 K. The catalyst with a dispersion of 0.36 gave a TOF of  $102 \text{ min}^{-1}$  at 548 K and 1 bar total pressure (inlet partial pressures of  $P_{gly} = 0.06$  bar,  $P_{H_2O} = 0.72$  bar, and  $P_{H_2} = 0.22$  bar). This value is 1.6 times greater than the value for the highly dispersed catalyst (dispersion = 0.53; TOF =  $67 \text{ min}^{-1}$ ), indicating slight structure sensitivity of the reaction. The trend was similar for the same reaction conditions at 498 K (14 and  $9 \text{ min}^{-1}$  for the poorly dispersed catalyst and highly dispersed catalyst, respectively). In addition, the ratio of TOF after reaction at 498 K to TOF before reaction at 498 K was 1.0 for the Pt-Re/C catalysts and 1.7 for the Pt/C catalysts (at inlet concentrations the same as for the Madon–Boudart criterion experiments with GHSV between  $7 \times 10^4$  and  $1 \times 10^5 \text{ h}^{-1}$ ). These results suggest that Re plays a role in stabilizing the catalyst surface.

Fig. 3 shows Arrhenius plots for the rates of glycerol conversion for the catalysts listed in Table 1. The Pt-Re catalyst with an atomic Pt:Re ratio of 1:2 had the highest TOF for CO production and an activation energy of  $70 \text{ kJ mol}^{-1}$ . Increasing the Pt:Re ratio to 1:1 decreased the TOF by a factor of 1.5. However, the activity was still 5 times higher than that of the monometallic Pt/C catalyst and the activation energy ( $60 \text{ kJ mol}^{-1}$ ) is similar to the Pt-Re (1:2) catalyst. The Pt-Re/C catalyst with an atomic Pt:Re ratio of 10:1 shows similar activity as the monometallic Pt catalyst, suggesting that the surface of this catalyst is similar to that of the Pt catalyst. The activation barrier over Pt/C ( $90 \text{ kJ mol}^{-1}$ ) is slightly higher than that over the Pt-Re catalysts. Fig. 4 shows that the reaction order with respect to glycerol pressure is approximately equal to 0.2 for the Pt-Re catalysts, and this reaction order appears to be near 0.1 for the monometallic Pt catalyst. By changing the inlet

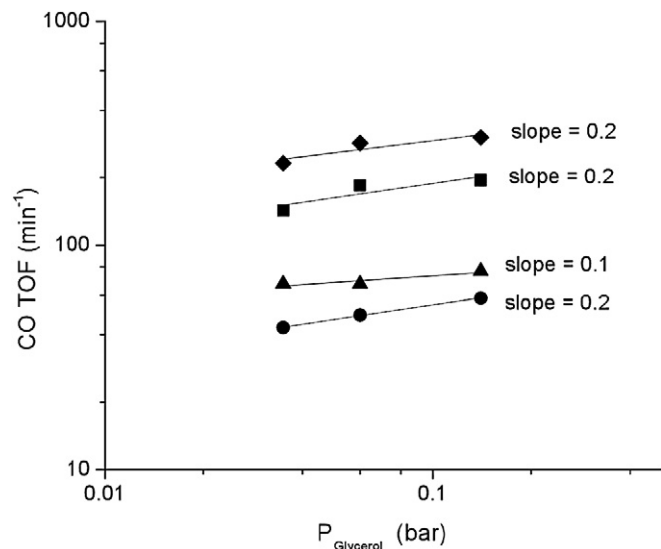


Fig. 4. Turnover frequency as a function of inlet glycerol partial pressure for Pt/C (▲), Pt-Re (10:1)/C (●), Pt-Re (1:1)/C (■), and Pt-Re (1:2)/C (◆) catalysts. Data collected at 548 K and inlet  $P_{H_2O} = 0.72$  bar (balance  $H_2$ ) over 30–50 mg of catalyst (GHSV between  $7 \times 10^4$  and  $1 \times 10^5 \text{ h}^{-1}$ ).

Table 2

$H_2$  and CO turnover frequencies (TOF) for Pt/C and Pt-Re/C at 498 K and 1 bar total pressure with inlet partial pressures of  $P_{gly} = 0.08$  bar and  $P_{H_2O} = 0.93$  bar over 760 mg Pt/C (GHSV =  $900 \text{ h}^{-1}$ ) and 97 mg Pt-Re/C (GHSV =  $7 \times 10^3 \text{ h}^{-1}$ )

Catalyst	CO TOF ( $\text{min}^{-1}$ )	$H_2$ TOF ( $\text{min}^{-1}$ )	Conversion to gas phase (%)
10 wt% Pt-Re (1:1)/C	12	17	24
5 wt% Pt/C	1.3	1.6	20

concentrations of  $H_2$  and water in a similar manner to the experiments in Fig. 4, the reaction order with respect to  $H_2$  was determined to be zero for all catalysts, and the order with respect to water was close to 0 (0.1) for the Pt:Re = 1:1 catalyst. To determine the  $H_2$  reaction order, the hydrogen partial pressure was varied from 0.075 to 0.24 bar for a glycerol pressure of 0.06 bar and a water pressure of 0.7 bar (balance He); and, to determine the  $H_2O$  reaction order, the water partial pressure was varied from 0.13 to 0.72 bar for a glycerol pressure of 0.06 bar (balance  $H_2$ ). The total pressure was equal to atmospheric pressure for all reaction kinetics experiments.

To probe the extent to which the presence of CO inhibits the rate of glycerol conversion, the 10 wt% Pt-Re (1:1)/C and 5 wt% Pt/C catalysts were tested at conditions leading to higher partial pressures of CO. In particular, whereas the above experiments were carried out using a  $H_2$  co-feed, which dilutes the CO that is produced during reaction, additional experiments were carried out at higher conversions (i.e., 20%) and without using a  $H_2$  co-feed. Table 2 shows the TOF for  $H_2$  and CO production for these 2 catalysts at 498 K over 24 h time on stream. The addition of Re to Pt increases the catalytic activity under these conditions by an order of magnitude. Importantly, under these conditions leading to high partial pressures of hydrogen, the catalysts were stable during the entire time on stream.

Analysis of the liquid effluent for reactions carried out at low conversions to the gas phase (i.e., <10% conversion, H<sub>2</sub> co-feed) over each catalyst showed >90 mol% of the carbon in the liquid phase was present as unconverted glycerol, with <5 mol% each of methanol, ethylene glycol, and acetol. For runs carried out at higher conversions to the gas phase without H<sub>2</sub> co-feed (i.e., ≥20% conversion to gas phase), the liquid effluents contained primarily unconverted glycerol, with 0.3–0.5 mol% methanol and 3–5 mol% acetol. The carbon balances for each set of conditions closed to within 10%.

## 4. Discussion

### 4.1. Formation of Pt–Re alloy

The reduction profile of the 5 wt% Pt/C catalyst is similar to that obtained by Zhang et al. for 2 wt% Pt/C, although they found a peak maximum near 390 K compared with our value near 450 K, probably the result of a slower temperature ramp rate (5 K min<sup>-1</sup>) used by Zhang et al. [24]. In this respect, Kanervo and Krause observed a similar shift of the reduction maximum to lower temperatures with decreasing heating rates for the TPR of CrO<sub>x</sub>/Al<sub>2</sub>O<sub>3</sub> and explain this phenomenon using a kinetic model [36]. Our peak maximum is in agreement with the value of 465 K obtained by Fraga et al. for reduction of a carbon-supported Pt catalyst [21].

Arnoldy et al. report a reduction maximum of 540 K for a catalyst consisting of 5.2 wt% Re (Re<sub>2</sub>O<sub>7</sub>) supported on activated carbon [37]. The discrepancy between this result and the reduction maximum for the Re/C catalyst studied in our work (636 K) may stem from different rhenium crystallite sizes for these samples which may result from differences in preparation procedures or rhenium salts used in catalyst preparation [37]. Hydrogen consumption measurements made by Arnoldy et al. are in agreement with our work and show the complete reduction of the precursor into metallic rhenium [37]. The presence of metallic rhenium in the reduced Re/C catalyst is further shown by sizable CO uptake after an isothermal reduction at 723 K. Arnoldy et al. suggest that reduction of the Re precursor on various supports proceeds in one step (Re<sup>7+</sup> → Re<sup>0</sup>) and is catalyzed by the presence of Re<sup>0</sup>, resulting in sharp reduction peaks [37]. The wider peak obtained in our reduction profiles may result from mass transfer limitations or heterogeneity of the Re surface species undergoing reduction.

The reduction maxima of the bimetallic catalysts appear to shift to lower temperatures with higher rhenium content. The reason for this shift may lie in the chlorine content of the catalysts before reduction. We observed that the amount of HCl released during TPR decreased with increasing rhenium content, such that a negligible amount of HCl was emitted during the reduction of the Pt–Re (1:2)/C catalyst. We suggest that addition of HReO<sub>4</sub> aids the release of chlorine, possibly as HCl during drying. Because no change in the oxidation state of either Pt or Re was detected by hydrogen consumption measurements after drying, it is possible that Cl ligands in [PtCl<sub>6</sub>]<sup>2-</sup> were partially or completely replaced by oxygen or hydroxyl species from the air, carbon surface groups, or HReO<sub>4</sub>, resulting in PtO<sub>x</sub>Cl<sub>y</sub> sur-

face species. Fraga et al. suggested a mechanism whereby the Cl ligands of H<sub>2</sub>PtCl<sub>6</sub> can be exchanged with hydroxyl groups of the support, yielding HCl without Pt reduction [21,38]. The increasing presence of PtO<sub>x</sub> may result in an earlier onset of reduction, because carbon-supported PtO<sub>2</sub> is known to reduce to metallic Pt at low temperatures [38]. This effect is particularly evident in the reduction profile of the Pt–Re (1:2)/C catalyst, which displays the earliest onset of reduction of the five catalysts studied.

The reduction profiles of the Pt–Re/C catalysts are all characterized by the simultaneous reduction of platinum and rhenium precursors, and the reduction peak occurs in the same region as that of the monometallic platinum catalyst (393–520 K). Various investigators have made similar observations for Pt–Re/Al<sub>2</sub>O<sub>3</sub> and agree that the shift in reduction temperature is an indication of Pt–Re alloy formation [39–42]. In other studies, Pt–Re alloy formation was verified for high-loading Pt–Re/C samples by X-ray diffraction studies [43] and by X-ray absorption for low-loading, highly dispersed Pt–Re/Al<sub>2</sub>O<sub>3</sub> catalysts [44]. Isaacs et al. suggested that on sufficiently hydrated Pt–Re/Al<sub>2</sub>O<sub>3</sub> catalysts, mobile rhenium oxide species can migrate toward reduced Pt particles, where Re reduction takes place [45]. Carbon is expected to have weaker metal–support interactions than refractory oxide supports [46], and it is likely that rhenium oxide species have high mobility on carbon and can come into intimate contact with reduced Pt centers to form bimetallic particles. Metallic Re can analogously catalyze the reduction of mobile Re oxides, and this mechanism may play an important role in the reduction of catalysts with high Re content (e.g., atomic Pt:Re = 1:2).

The diffraction pattern of the 10 wt% Pt–Re (1:1)/C catalyst reduced at 723 K for 2 h did not contain any peaks, indicating that at this reduction temperature, metal particles were too small to produce coherent reflections. This observation is in agreement with the metal particle size of 3.8 nm as calculated from CO-chemisorption measurements and the equation for atomic density of (111) planes ( $d_p = 1.1/\text{Dispersion}$ , where  $d_p$  is the particle diameter in nm). A sintering treatment consisting of reduction at 973 K for 12 h yielded a catalyst with diffraction patterns containing peaks at  $2\theta = 37.6^\circ, 40.4^\circ, 46.2^\circ, 67.8^\circ$ , and  $81.9^\circ$ . This pattern closely matched the pattern obtained by Anderson et al. for 20 wt% Pt–Re (1:1)/C catalyst; those authors concluded that this pattern suggests the presence of a mixture of hcp and fcc Pt–Re alloy crystals, with the absence of unalloyed Pt and Re [43]. The presence of both fcc and hcp phases is consistent with the Pt–Re phase diagram, which predicts the coexistence of Pt-rich fcc and Re-rich hcp phases for overall Pt atomic fractions of 40–63% [47].

The results from our chemisorption measurements also indicate the formation of Pt–Re alloys. Our result of negligible H<sub>2</sub> uptake on Re/C is in agreement with similar studies of alumina-supported Re [25,48–50]; Yao and Shelef attributed this behavior to the inability of dispersed Re to dissociate H<sub>2</sub> [50]. The suppression of H<sub>2</sub> uptake by the addition of Re to catalysts with the same Pt content is in agreement with other studies of Pt–Re/Al<sub>2</sub>O<sub>3</sub> [25,42,51]. Isaacs and Petersen suggested that because Re does not chemisorb H<sub>2</sub>, the H<sub>2</sub> uptake of a Pt–Re

catalyst should be the same as that of monometallic Pt if there is no metal interaction [25]. However, their results showed a greater than twofold decrease in H<sub>2</sub> uptake on the addition of an equal mass of Re to Pt/Al<sub>2</sub>O<sub>3</sub>, which suggests a close interaction between Pt and Re [25]. Furthermore, Prestvik et al. and Fernández-García et al. reported suppression of H<sub>2</sub> uptake for bimetallic Pt–Re alloy catalysts [42,51]. Our results show a twofold decrease in H<sub>2</sub> uptake with the addition of an equimolar amount of Re to Pt/C, similar to the result of Isaacs and Petersen [25], again suggesting the formation of an alloy for our Pt–Re/C catalysts.

#### 4.2. Kinetics of glycerol conversion and the effect of Re

In previous work, Cortright et al. showed that H<sub>2</sub> can be produced via aqueous-phase reforming (APR) of oxygenated hydrocarbons, including glycerol, over Pt-based catalysts, and proposed a mechanism whereby the oxygenated molecule adsorbs on Pt by dehydrogenation, followed by C–C bond cleavage to give H<sub>2</sub> and adsorbed CO [2]. Because APR occurs at high total pressure and high partial pressures of water, the adsorbed CO species then reacts with water via the WGS reaction to form CO<sub>2</sub> and H<sub>2</sub> [2]. We suggest that glycerol conversion under our vapor-phase conditions occurs via a similar mechanism as for APR. However, our reaction occurs at lower total pressure, resulting in a decreased partial pressure of water in our system compared with the APR process. Under APR reaction conditions, the WGS reaction is nearly equilibrated [5], whereas at the reaction conditions of the present study, the WGS reaction is far from equilibrium, and the final products are primarily CO and H<sub>2</sub>. Catalyst support also plays an important role with respect to the WGS reaction, and in previous work we showed that metal-oxide-supported Pt catalysts have higher WGS activity compared with the carbon-supported catalyst [17]. The Al<sub>2</sub>O<sub>3</sub> support used in the APR studies likely contributes to the WGS activity.

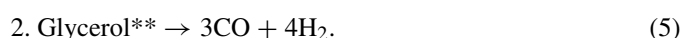
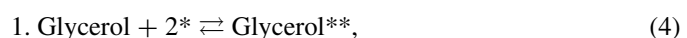
Shabaker et al. carried out reaction kinetic studies of the APR of oxygenated hydrocarbons over Pt/Al<sub>2</sub>O<sub>3</sub> and showed that the reaction to form CO<sub>2</sub> and H<sub>2</sub> is fractional order with respect to the oxygenated hydrocarbon feed molecule (0.4) [5], and the reaction has an apparent activation barrier of 110 kJ mol<sup>-1</sup> [6]. These results are similar to those in our study. The fact that the conversion of glycerol to synthesis gas is fractional order with respect to glycerol (0.1) indicates that the coverage of glycerol-derived adsorbed species on Pt/C is significant under our reaction conditions, similar to APR of ethylene glycol [5]. The activation barrier to produce CO over our Pt/C catalyst (90 kJ mol<sup>-1</sup>) is similar to that for APR of ethylene glycol over Pt/Al<sub>2</sub>O<sub>3</sub> as well. These results suggest that the conversion of glycerol to synthesis gas has similar kinetics as the APR of ethylene glycol. Accordingly, both reactions appear to be kinetically limited by the rate of CO formation, because the WGS reaction is not significant under the conditions of the present study and the rate of WGS is reversible under APR reaction conditions. Shabaker et al. showed that the rate of APR for ethylene glycol is inhibited by H<sub>2</sub> due to blockage of surface sites by adsorption of atomic hydrogen [5]. In contrast, our

results for glycerol conversion indicate that the reaction is zero-order with respect to H<sub>2</sub>. This difference is probably caused by higher surface coverages by adsorbed CO in our case, because adsorbed CO is removed from the surface (as CO<sub>2</sub>) by the WGS reaction during APR conditions, whereas CO must desorb from the surface under our reaction conditions for glycerol conversion, leading to high concentrations of CO in the gas stream.

In our previous work dealing with glycerol conversion to CO and H<sub>2</sub> [17], we suggested that the low activity of Pt/C at temperatures below 573 K was caused by surface site blocking by strongly adsorbed CO, and the addition of Re to the Pt/C catalyst was necessary to weaken the binding energy of CO on Pt, thus increasing the rate at lower temperatures. Therefore, higher rates could be expected at low conversion conditions and with the co-feeding of H<sub>2</sub>, because both of these situations correspond to lower CO partial pressures (thus favoring CO desorption from the surface). Under these conditions, the addition of an equal molar amount of Re to Pt/C increases the rate of CO production by a factor of 5. However, under conditions where CO blocking of surface sites is expected to be more severe (i.e., 498 K, 20% conversion to gas phase, and without H<sub>2</sub> co-feeding), this same addition of Re increases the rate by an order of magnitude. The reaction order with respect to glycerol is unaffected by Re, and the activation barrier decreases slightly. These results suggest that the primary effect of Re on the kinetics of the conversion of glycerol to synthesis gas over Pt is in fact to weaken the interaction of CO with the surface.

Fundamental and theoretical studies of CO adsorption on Pt–Re alloy surfaces indicate a weakening in the Pt–CO binding strength with the addition of Re. Temperature-programmed desorption (CO-TPD) experiments performed by Ramstadt et al. for a Re-doped Pt(111) surface show a shift of the CO desorption peak maximum to lower temperatures with increasing surface rhenium content [52]. In a DFT study, Ishikawa et al. reported a 35% decrease in the calculated CO binding energy of a Pt–Re(111) surface compared with Pt(111) [53]. Greeley et al. reported a similar decrease in CO binding energy for Pt over-layers on bulk Re [54]. These studies support the suggestion that the promoting effect of Re on Pt for glycerol conversion to synthesis gas is related to a weakening of the interaction of CO with the surface, allowing the catalyst to operate at high rates at conditions leading to high CO partial pressures, that is, at high reactant conversions and without a H<sub>2</sub> co-feed.

In an effort to describe more quantitatively the effects of CO on the rate of glycerol conversion over Pt and Pt–Re catalysts, we developed the simplified mechanism shown below, involving adsorption of glycerol followed by a surface reaction step in which adsorbed glycerol undergoes irreversible reaction (e.g., cleavage of a C–C bond), eventually leading to gaseous CO and H<sub>2</sub>, where \* is a vacant site and Glycerol\*\* is adsorbed glycerol:



The second step is a lumped process involving a series of reactions leading to CO and H<sub>2</sub>. The first of these reactions is assumed to be irreversible cleavage of the C–C bond, and thus

Table 3

Model parameters and comparison of predicted conversion and CO TOF to experimental results

Catalyst	Experimental conversion (%)	Predicted conversion (%)	Experimental CO TOF (min <sup>-1</sup> )	Predicted CO TOF (min <sup>-1</sup> )	$k_2$ (min <sup>-1</sup> )	$K_{CO}$ (atm <sup>-1</sup> )	$\alpha$ (atm <sup>-1</sup> )
Pt/C	4.9 <sup>a</sup>	5.5	8.7 <sup>a</sup>	10	7500	55000	800
Pt/C	20 <sup>b</sup>	14	1.3 <sup>b</sup>	1.2	7500	55000	800
Pt–Re/C	7.5 <sup>a</sup>	8.8	46 <sup>a</sup>	58	1000	5000	800
Pt–Re/C	24 <sup>b</sup>	18.6	12 <sup>b</sup>	11	1000	5000	800

The predicted reaction order with respect to glycerol was 0.3. Conversion calculated as ( $C_{out}$  in gaseous products)/(total C fed to reactor as glycerol)  $\times 100$ .

<sup>a</sup> Reaction conditions as in Fig. 3.

<sup>b</sup> Reaction conditions as in Table 2.

all steps following this irreversible cleavage are kinetically insignificant. In addition, we note that the surface is undoubtedly covered by adsorbed CO, glycerol, H, and OH species; however, adsorbed CO and glycerol are assumed to be the dominant surface species, and the coverages of H and OH are thus assumed to be insignificant (i.e., the site balance contains only adsorbed CO, glycerol, and vacant sites). This simplified reaction scheme gives the following rate expression, which depends on three parameters: the rate constant of step 2 ( $k_2$ ), the CO adsorption equilibrium constant ( $K_{CO}$ ), and a grouping of the forward and reverse rate constants of step 1 with the rate constant of step 2 [ $\alpha = k_1/(k_{-1} + k_2)$ ]:

$$r = k_2 \alpha P_G \theta_*^2, \quad (6)$$

$$\theta_* = \frac{-(1 + K_{CO} P_{CO}) + \sqrt{(1 + K_{CO} P_{CO})^2 + 8\alpha P_G}}{4\alpha P_G}, \quad (7)$$

where  $P_{CO}$  and  $P_G$  are the partial pressures of CO and glycerol, respectively. Keeping the value of  $\alpha$  the same for both Pt/C and Pt–Re/C, this simple kinetic model describes the changes in rate at 498 K for both Pt/C and Pt–Re (1:1)/C catalysts caused by changing from conditions of low conversion using a  $H_2$  co-feed stream to conditions of higher conversion and without using a  $H_2$  co-feed stream (Table 3). According to this simple model, the value of  $K_{CO}$  is 10 times lower for Pt–Re/C compared with Pt/C, whereas the value of  $k_2$  is 8 times higher for Pt/C compared with Pt–Re/C. The parameter values for each catalyst are listed in Table 3. Importantly, this model can be useful in future scale-up of the glycerol system to achieve higher conversions for coupling with subsequent Fischer–Tropsch synthesis.

## 5. Conclusion

TPR studies for Pt/C, Pt–Re/C, and Re/C catalysts suggest that the presence of Pt catalyzes the reduction of Re, leading to the formation of Pt–Re alloys supported on carbon. Chemisorption and XRD experiments support the result of alloy formation for Pt–Re/C catalysts. Reaction kinetics measurements at 498–548 K for the conversion of glycerol to synthesis gas in the vapor phase over Pt/C and Pt–Re/C catalysts showed that stable catalyst performance could be achieved at low conversions by co-feeding  $H_2$ . The rate of glycerol conversion under these conditions is controlled by the intrinsic reaction kinetics and is free from transport limitations, as determined from the Madon–Boudart criterion. Under these reaction conditions, bimetallic

Pt–Re/C catalysts with atomic Pt:Re  $\leq 1$  are 5 times more active than monometallic Pt/C and Pt–Re with a higher Pt:Re ratio (10:1). The reaction order with respect to glycerol was fractional over all catalysts, and the activation energy was 60–90 kJ mol<sup>-1</sup>. The reaction order with respect to the oxygenated feed molecule and the activation barrier to final products determined in this study for glycerol conversion to synthesis gas over Pt/C are similar to those for the APR of ethylene glycol to  $CO_2$  and  $H_2$  over Pt/Al<sub>2</sub>O<sub>3</sub>. However, whereas the APR of ethylene glycol to  $CO_2$  and  $H_2$  is negative order with respect to the hydrogen pressure, the rate of glycerol conversion to CO and  $H_2$  in the vapor phase is zero order in hydrogen. In addition, glycerol conversion to synthesis gas is inhibited by CO, with lower rates at higher conversions and without a  $H_2$  co-feed. Importantly, the rate of glycerol conversion under these conditions over Pt–Re/C is an order of magnitude higher than the rate over Pt/C, suggesting that the primary promotional effect of Re is to weaken the interaction of CO with the surface, thereby lowering the CO coverage and allowing the catalyst to operate at high rates under conditions leading to high CO pressures.

## Acknowledgments

This work was supported by the US Department of Energy (DOE), Office of Basic Energy Sciences, Chemical Sciences Division. We thank Alexandar Peykov for assistance in collecting reaction kinetics data, Drew Braden for assistance with kinetic modeling, Ricardo Soares for helpful discussions regarding TPR, and Manos Mavrikakis for valuable discussions and collaborations throughout this entire project.

## References

- [1] D.L. Klass, Biomass for Renewable Energy, Fuels, and Chemicals, Academic Press, San Diego, 1998.
- [2] R.D. Cortright, R.R. Davda, J.A. Dumesic, *Nature* 418 (2002) 964.
- [3] R.R. Davda, J.A. Dumesic, *Chem. Commun.* 1 (2004) 36.
- [4] R.R. Davda, J.W. Shabaker, G.W. Huber, R.D. Cortright, J.A. Dumesic, *Appl. Catal. B* 43 (2003) 13.
- [5] J.W. Shabaker, R.R. Davda, G.W. Huber, R.D. Cortright, J.A. Dumesic, *J. Catal.* 215 (2003) 344.
- [6] J.W. Shabaker, J.A. Dumesic, *Ind. Eng. Chem. Res.* 43 (2004) 3105.
- [7] J.W. Shabaker, G.W. Huber, R.R. Davda, R.D. Cortright, J.A. Dumesic, *Catal. Lett.* 88 (2003) 1.
- [8] J.W. Shabaker, G.W. Huber, J.A. Dumesic, *J. Catal.* 222 (2004) 180.
- [9] E. Chornet, D. Wang, S. Czernik, D. Montane, M. Mann, in: Proc. 1996 U.S. DOE Hydrogen Prog. Rev., Miami, FL, 1996.

- [10] S. Czernik, R. French, C. Feik, E. Chornet, *Ind. Eng. Chem. Res.* 41 (2002) 4209.
- [11] D. Wang, S. Czernik, E. Chornet, *Energy Fuels* 12 (1998) 19.
- [12] D. Wang, S. Czernik, D. Montane, M. Mann, E. Chornet, *Ind. Eng. Chem. Res.* 36 (1997) 1507.
- [13] M. Asadullah, S. Ito, K. Kunimori, M. Yamada, K. Tomishige, *J. Catal.* 208 (2002) 255.
- [14] T. Wang, J. Chang, P. Lv, *Energy Fuels* 19 (2005) 637.
- [15] G.W. Huber, J.N. Chheda, C.J. Barrett, J.A. Dumesic, *Science* 308 (2005) 1446.
- [16] G.W. Huber, R.D. Cortright, J.A. Dumesic, *Angew. Chem. Int. Ed.* 43 (2004) 1549.
- [17] R.R. Soares, D.A. Simonetti, J.A. Dumesic, *Angew. Chem. Int. Ed.* 45 (2006) 3982.
- [18] C.H. Bartholomew, R.J. Farrauto, *Fundamentals of Industrial Catalytic Processes*, Wiley, Hoboken, NJ, 2006.
- [19] B.E. Spiewak, J. Shen, J.A. Dumesic, *J. Phys. Chem.* 99 (1995) 17640.
- [20] S.R. de Miguel, O.A. Scelza, M.C. Roman-Marinez, C. Salinas-Martinez, *Appl. Catal. A* 170 (1998) 93.
- [21] M.A. Fraga, E. Jordao, M.J. Mendes, M.M.A. Freitas, J.L. Faria, J.L. Figueiredo, *J. Catal.* 209 (2002) 355.
- [22] A. Guerrero-Ruiz, P. Badenes, I. Rodriguez-Ramos, *Appl. Catal. A* 173 (1998) 313.
- [23] A. Sepulveda-Escribano, F. Coloma, F. Rodriguez-Reinoso, *Appl. Catal. A* 173 (1998) 247.
- [24] Y.J. Zhang, A. Maroto-Valiente, I. Rodriguez-Ramos, X. Qin, A. Guerrero-Ruiz, *Catal. Today* 93–95 (2004) 619.
- [25] B.H. Isaacs, E.E. Petersen, *J. Catal.* 85 (1984) 1.
- [26] J.B. Anderson, *Chem. Eng. Sci.* 18 (1963) 147.
- [27] J.J. Carberry, *AIChE J.* 7 (1961) 350.
- [28] G.F. Froment, K.B. Bischoff, *Chemical Reactor Analysis and Design*, Wiley, New York, 1990.
- [29] D.E. Mears, *J. Catal.* 20 (1971) 127.
- [30] D.E. Mears, *Ind. Eng. Chem. Process Des. Dev.* 10 (1971) 541.
- [31] C.N. Satterfield, *Mass Transfer in Heterogeneous Catalysis*, MIT Press, Cambridge, MA, 1970.
- [32] J.M. Smith, *J. Chem. Eng. Jpn.* 6 (1973) 191.
- [33] P.B. Weisz, *Z. Phys. Chem.* 11 (1957) 1.
- [34] P.B. Weisz, C.D. Prater, *Adv. Catal.* 6 (1954) 143.
- [35] R.J. Madon, M. Boudart, *Ind. Eng. Chem. Fund.* 21 (1982) 438.
- [36] J.M. Kanervo, A.O.I. Krause, *J. Phys. Chem. B* 105 (2001) 9778.
- [37] P. Arnoldy, E.M. van Oersa, O.S.L. Bruinsma, V.H.J. de Beer, J.A. Moulijn, *J. Catal.* 93 (1985) 231.
- [38] S.Y. Huang, S.M. Chang, C.T. Yeh, *J. Phys. Chem. B* 110 (2006) 234.
- [39] S.M. Augustine, W.M.H. Sachtler, *J. Catal.* 116 (1989) 184.
- [40] C. Bolivar, H. Charcosset, R. Frety, M. Primet, L. Tournayan, C. Betizeau, G. Leclercq, R. Maurel, *J. Catal.* 39 (1975) 249.
- [41] C. Laiyuan, N. Yueqin, Z. Jinling, L. Liwu, L. Xihui, C. Sen, *J. Catal.* 145 (1994) 132.
- [42] R. Prestvik, K. Moljord, K. Grande, A. Holmen, *J. Catal.* 174 (1998) 119.
- [43] A.D. Anderson, G.A. Deluga, J.T. Moore, M.J. Vergne, D.M. Hercules, E.A. Kenik, C.M. Lukehart, J. Nanosci. Nanotechnol. 4 (2004) 809.
- [44] M. Ronning, T. Gjervan, R. Prestvik, D.G. Nicholson, A. Holmen, *J. Catal.* 204 (2001) 292.
- [45] B.H. Isaacs, E.E. Petersen, *J. Catal.* 77 (1982) 43.
- [46] J. Phillips, J. Weigle, M. Herskowitz, S. Kogan, *Appl. Catal. A* 173 (1998) 273.
- [47] T.B. Massalski, *Binary Alloy Phase Diagrams*, ASM International, 1992.
- [48] C. Bolivar, H. Charcosset, R. Frety, M. Primet, L. Tournayan, C. Betizeau, G. Leclercq, R. Maurel, *J. Catal.* 45 (1976) 163.
- [49] J. Freel, *Prepr. Am. Chem. Soc. Div. Pet. Chem.* 18 (1973) 10.
- [50] H.C. Yao, M. Shelef, *J. Catal.* 44 (1976) 392.
- [51] M. Fernández-García, F.K. Chong, J.A. Anderson, C.H. Rochester, G.L. Haller, *J. Catal.* 182 (1999) 199.
- [52] A. Ramstad, B. Strisland, S. Raaen, A. Borg, C. Berg, *Surf. Sci.* 440 (1999) 290.
- [53] Y. Ishikawa, M.S. Liao, C.R. Cabrera, *Surf. Sci.* 513 (2002) 98.
- [54] J. Greeley, M. Mavrikakis, *Catal. Today* 111 (2005) 52.